THE JOURNAL OF PHYSICAL CHEMISTRY C

Article

Cite This: J. Phys. Chem. C 2018, 122, 26499−26505

pubs.acs.org/JPCC

Magnetic-State Controlled Molecular Vibrational Dynamics at Buried Molecular−Metal Interfaces

Isidoro Martinez,[†,▽] Juan Pedro Cascales,[†,‡,▽] Cesar Gonzalez-Ruano,[†] Jhen-Yong Hong,[§,∥] Chen-Feng Hung,[§] Minn-Tsong Lin,[§,⊥] Thomas Frederiksen,[#,¶] and Farkhad G. Aliev[†,*]

[†]Departamento Fisica Materia Condensada, C03, IFIMAC and INC, Universidad Autonoma de Madrid, 28049 Madrid, Spain

[‡]Francis Bitter Magnet Laboratory, Massachusetts Institute of Technology, Cambridge, Massachusetts 02139, United States

[§]Department of Physics, National Taiwan University, Taipei 10617, Taiwan

[∥]Department of Physics, Tamkang University, New Taipei City 25137, Taiwan

[⊥]Institute of Atomic and Molecular Sciences, Academia Sinica, Taipei 10617, Taiwan

[#]Donostia International Physics Center (DIPC), E-20018 Donostia-San Sebastián, Spain

[¶]IKERBASQUE, Basque Foundation for Science, E-48013 Bilbao, Spain

Supporting Information

ABSTRACT: Self-assembled molecular (SAM) structures have been intensively used in molecular electronics and spintronics. However, detailed nature of the interfaces between molecular layers and extended metallic contacts used to bias the real devices remains unclear. Buried interfaces greatly restrict the application of standard techniques such as Raman or scanning electron microscopy. Here, we introduce low-frequency noise spectroscopy as a tool to characterize buried molecular−metal interfaces. We take advantage of vibrational heating of the molecules with incomplete contacts to the interface. Electrons, being the main spin and charge carriers propagating through the interfaces involving SAMs, interact inelastically with the nuclei and excite quantum molecular vibrations (phonons). Our detailed investigation of both conductance and conductance fluctuations in magnetic tunnel junctions with few nanometer perylenetetracarboxylic dianhydride (PTCDA) allows to map vibrational heating at specific biases taking place in hot spots such as where SAM layers make unstable contact to the metallic electrodes. We follow this effect as a function of PTCDA thickness and find the highest molecular−metal order for the lowest (three to five monolayers) barriers. Moreover, we show experimentally that the low-frequency noise depends on the relative alignment of electrodes well beyond expectations from fluctuation−dissipation theorem. In combination with modeling, we interpret this effect as due to a magnetic-state dependent molecular vibrational heating at the interfaces driven by the spin-polarized current.

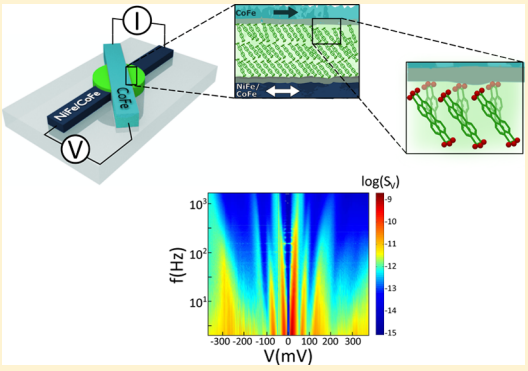

1. INTRODUCTION

Downscaling of inorganic electronics has currently become increasingly difficult because of physical limitations, due to surface-related modification of electronic structures. The bottom-up concept introduced by molecular electronics in order to solve the problem has been around since the seventies,[1] and unique intrinsic features of molecules and quantum dots, among other excited phonons and vibrations,[2−4] have been explored intensively.

One of the major challenges in molecular electronics (molecular spintronics) is control over molecules−metal (ferromagnetic electrodes) contacts.[5] To avoid possible damage to molecular order and even pinhole formation, deposition of seed underoxidized atomic thickness alumina layer has been proposed.[6] This method improves the interface quality, reduces the influence of conductance mismatch, and enhances the spin life time.[6,7] However, as long as one deals with buried interfaces, the tools available to evaluate their quality are very limited. For such purpose (when electron transmission microscopy is used[8]), the device is usually destroyed.

Electron transport through the interfaces could be a nondestructive, albeit indirect method to evaluate buried molecule−metal interface quality. Few main factors determine transport in molecular electronics, with electron−phonon coupling being important along with molecular and electrode electronic structures.[9−11] Identification of phonon modes is usually carried out by Raman or inelastic tunneling spectros-

Received: September 12, 2018
Revised: October 29, 2018
Published: October 30, 2018

DOI: 10.1021/acs.jpcc.8b08913
J. Phys. Chem. C 2018, 122, 26499−26505

copy (IETS).[11,12] Because of strong photon attenuation by the metallic electrodes, Raman spectroscopy on heterostructures mainly reflects information from the outer surface layers.[13]

The IETS technique, based on a weak change in the tunneling conductance beyond the vibrational onsets of excitation, was originally developed for metal−metal oxide−metal junctions[14] and later extended to explore molecular vibrations in the single-molecule limit[15,16] or investigation of atomic scale magnetism[17,18] using scanning tunneling microscopy. For organic magnetic tunnel junctions (OMTJs), the conductance signals are averaged over a large number of molecules forming either barrier or contacting extended ferromagnetic electrodes. To the best of our knowledge, the only study of IETS in molecular spintronics with laterally extended ferromagnetic electrodes just aimed to obtain structural information on the integrity of the organic semiconducting barrier by localizing junctions with pinholes where no signatures of molecular vibrational modes were present.[12] As shown here, for high-quality buried molecular−metal interfaces with only a small percentage of the molecules weakly contacting the electrodes, signatures arise that can be understood in terms of vibrational heating of the molecules in locally distributed hot spots.

Vibrational heating (or cooling) of the molecules contacting metal electrodes is a well-established phenomenon[19] for atomic and molecular junctions. Vibrational heating at finite bias is among the major obstacles for advances in molecular electronics and spintronics because of the associated potential device breakdown.[3,19−21] Peculiarly, as mentioned above, a current flux can either heat or cool locally the molecular junction close to subvibration resonance conditions.[20,22]

Inclusion of electron spin degree of freedom in OMTJs[6,23−30] and interface-related molecular magnetism[31,32] potentially allows spin control over vibrons, as pointed out in recent theoretical studies.[33,34] Other theories go even further and predict phonon-dressed spins to exist with effective magnetic moments of 0.024 μ_B for single-phonon quanta with the original system being nonmagnetic.[35] The interplay between spins and phonons in molecular spintronics remains however obscured.

As we shall see below, the conductance fluctuations or inelastic noise probing vibron excitations could present an alternative tool capable of identifying high-quality buried molecules−metal interfaces. At low temperatures and biases not yet exciting molecular vibrations or defect states (e.g., typically below 10 mV), voltage fluctuations are dominated by shot noise providing information on interfacial electron−electron correlations.[36] At higher biases (typically exceeding phonon energies situated above 15 mV), the low-frequency noise (LFN) is known to provide unique capability of identifying surface-located molecules through their vibrations in nonspintronic systems.[37,38]

Here, we describe a qualitative step further and introduce vibron noise spectroscopy, which addresses the challenge of investigating the quality of buried molecular−metal (ferromagnet) interfaces in OMTJs. Our experiments monitor conductance, tunneling magnetoresistance (TMR), and voltage fluctuations as a function of applied bias and magnetic state in OMTJs with efficient heat transport away from the molecules so that the structure of junction is not jeopardized. Junctions with the thinnest [3−5 perylenetetracarboxylic dianhydride (PTCDA) monolayers] barrier show the smallest background noise and highest TMR of 20−30% indicative of their major structural order. In those junctions, we experimentally observe and theoretically model the magnetic-state dependent molecular vibrational dynamics. The physical origin of this effect is related to the difference of available phase space for the inelastic tunneling process between parallel (P) and antiparallel (AP) states. Besides, our results open the possibility of spin heat dissipation control in molecular spintronics.

2. EXPERIMENTAL SECTION

2.1. Sample Growth. The layer sequence in the PTCDA organic spin valves studied in this work is NiFe(25 nm)/CoFe(15 nm)/Al_xO(0.6 nm)/PTCDA(1.2−5 nm)/Al_xO(0.6 nm)/CoFe(30 nm). The structure was deposited onto a glass substrate, and the junctions were prepared in a high-vacuum environment with a base pressure lower than 10^{-8} mbar. The metallic layers were deposited by sputtering with an Ar working pressure of 5×10^{-3} mbar. The PTCDA layers were grown by thermal evaporation at 10^{-8} mbar, with a deposition rate of 0.1 nm/s. Thin AlO_x layers were grown between the PTCDA layer and both ferromagnetic layers by partially oxidizing Al in an oxygen plasma for 5 s.

2.2. Electron Transport and Noise Measurements. Electron transport and noise were measured down to 0.3 K using a He-3 JANIS cryostat. LFN experiments were carried out using a Stanford Research SR785 spectrum analyzer. The signal is duplicated into two channels identically amplified in two stages in order to use a cross-correlation technique, so we may neglect extrinsic voltage noise contributions. We analyze the variation of LFN by direct plots of noise power. For the qualitative comparison of the frequency-averaged LFN levels in our OMTJs with PTCDA barrier thickness, we also used the Hooge factor α defined[40] via $S_V(f) = \alpha V^2/Af^\beta$, where V is the bias voltage, A the junction area, f the frequency, and β a parameter close to 1. More details regarding the growth and measurement technique can be found in refs.[7,36,39,40]

3. RESULTS

Figure 1 illustrates the investigated OMTJs highlighting the 1.2 nm thick barrier cross section (with approximately three layers of PTCDA). The sketched molecular order (zoom in Figure 1a) describes a realistic PTCDA structure with some conductance channels at zero bias being open due to molecular bending, interface roughness, or local disorder.

An exponential dependence of the room-temperature conductance with the PTCDA thickness[36] and a large TMR (Figure 1b,c) indicate that the electron transport through the PTCDA layer is dominated by direct tunneling with energy and spin relaxation close to the molecule/ferromagnet interfaces. Figure 1b shows two well-defined and reproducible magnetic states corresponding to P and close to AP alignment of the electrodes. TMR values (up to 30%) observed with below 2 nm thick PTCDA barriers (three to five monolayers) are among the highest reported so far in molecular spintronic junctions in the tunneling regime. High TMR signals well ordered self-assembled thinnest PTCDA barrier. Conductance and noise in a total of 13 samples were investigated with PTCDA thickness ranging from 0 to 6 nm. Unless otherwise indicated, the measurement temperature is 10 K.

Figure 2a−c describes the representative behavior of noise for OMTJs with a PTCDA thickness of 1.2 nm in two magnetic states. These junctions show the lowest contribution

DOI: 10.1021/acs.jpcc.8b08913
J. Phys. Chem. C 2018, 122, 26499−26505

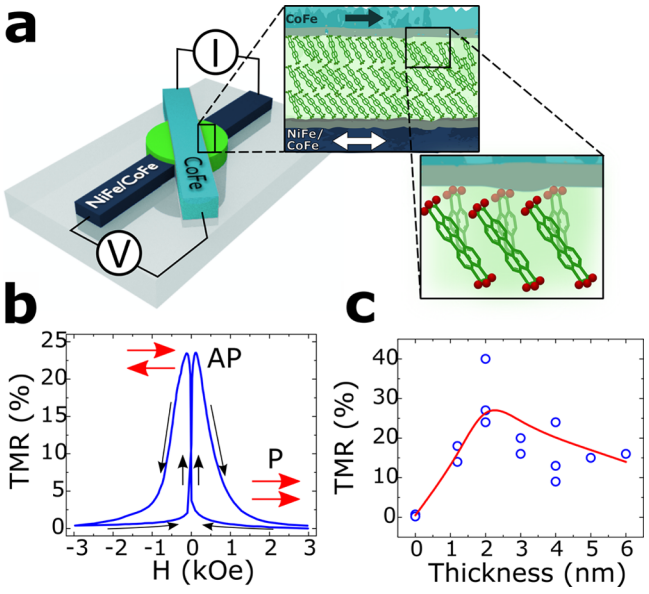

Figure 1. (a) Sketch of the junction structure and zoom of the cross section of PTCDA barrier highlighting the possible molecular bond rattling due to interface roughness. (b) Typical low-bias (0.7 mV) TMR measured in OMTJs with a 2 nm thick barrier at 10 K. Red arrows indicate P and AP states while dotted black arrows show magnetic field sweep directions. (c) Dependence of the low-bias TMR (T = 10 K) on the PTCDA thickness in OMTJs. The red curve is a guide for the eye.

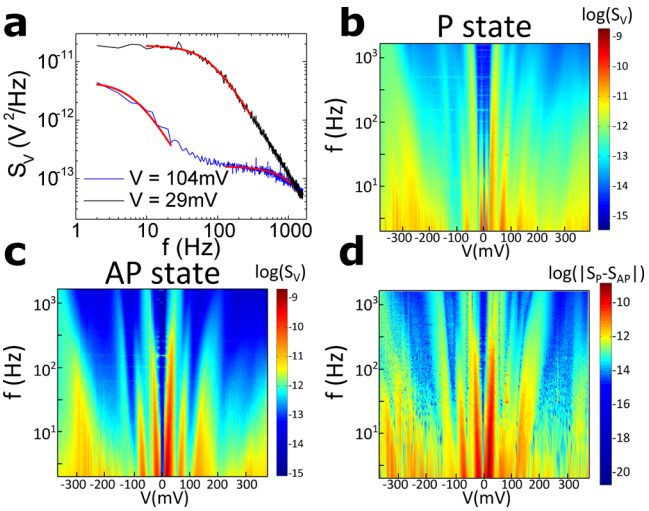

Figure 2. Part (a) shows the LFN spectra for two different biases close to the range with excess RTN with fit to a Lorentzian function (red curves). Parts (b,c) show the bias-dependent LFN in the junction with 1.2 nm PTCDA at P and AP states, respectively. Finally, part (d) shows the absolute value of the difference of noise power in two magnetic states. The measurements have been carried out at T = 10 K.

to the $1/f$ noise signaling a higher molecular order. One observes unexpected enhancement of the noise power due to appearance of random telegraph noise (RTN) in conductance close to a set of specific biases. Qualitatively similar magnetic-state dependent LFN has been found when the measurements are carried out at a base temperature of T = 0.3 K (Figure S1 in the Supporting Information). Decreasing the temperature from 10 to 0.3 K opens a low bias gap of about 20 mV for RTN excitation and generally reduces the amplitude of the LFN anomalies without qualitative changes relative to the data obtained at 10 K. We attribute that change to the possible excitation of collective molecular vibrations (librons) when temperatures exceed tens of K. Therefore, our IETS noise spectroscopy should mainly operate at low temperature, if one targets dynamics of the individual interfacial molecules. The close to symmetric character of the LFN anomalies with voltage V points toward a *inelastic origin* rather than to a resonant electron tunneling process, for which LFN enhancement is expected for one bias polarity only.[41]

In order to analyze in detail the shape and symmetry of the RTN on bias, the observed effect has been represented in two qualitatively different plots. From the one side, Figure 2b shows rough data, that is, the variation of the noise power in the parallel state (S_P) with frequency and the applied bias. On the other hand, we have quantified how RTN characteristic frequency varies with applied bias and its polarity. As an example, Figure 2a shows cross sections of $S_P(f,V)$ from Figure 2b for the two particular biases close revealing specific RTN *humps*. With increasing bias, the RTN first appears as a noise excess in the low-frequency limit which approximately varies as $1/(f^2 - f_0^2)$ with f_0 being the characteristic RTN frequency. This quantitative analysis confirms that the set of specific RTN excitations is *nearly symmetric in bias* and shows an increase of f_0 under the applied bias before RTN disappears outside the experimental bandwidth. Some asymmetry could probably be related with differences in the bottom and top electrode roughness and electrode/barrier interface.

Interestingly, switching the device with clear LFN anomalies (here with PTCDA ≤2 nm as we shall see below) to the AP state substantially changes the LFN (Figure 2c). In order to quantify the net change in LFN between the two magnetic states, we calculate the absolute value of the difference of the noise power between P and AP states $|S_P - S_{AP}|$ (Figure 2d). Note that for both magnetic states and at biases exceeding 200 mV, the RTN anomalies appear to be smeared out. As seen in Figure 2b,c and specially for OMTJs with yet thicker PTCDA, in the high-bias range, the so-called $1/f$ background noise becomes superimposed on the RTN contribution, making it more challenging to accurately determine the RTN frequency f_0.

In order to better understand the nature of the observed bias and magnetic-state dependent RTN, we carried out noise spectroscopy as a function of PTCDA thickness (see Figure 3). Let us first analyses LFN in the control samples (i.e., junctions without PTCDA but with 0.6 + 0.6 nm of AlO_x separating two ferromagnetic electrodes). One observes practically featureless background noise (Figure 3a), which is at least 2 orders of magnitude below the LFNs measured in any of the junctions with a PTCDA barrier. We conclude that the set of the bias-dependent RTN features originates from molecular vibrations inside the PTCDA barrier or at the PTCDA/electrode interfaces.

A further increase of the PTCDA thickness maintains the well-defined bias-dependent RTN anomalies only for barrier thickness below or about 2 nm. We observe the clear signatures of vibron-related LFNs with 1.2 nm and partially with 2 nm PTCDA thickness only. The further increase of the PTCDA thickness (as shown for OMTJ with 4 nm PTCDA) smears out vibron-related signatures in noise because of the onset of strong background $1/f$ noise already at relatively small biases (Figure 3c).

DOI: 10.1021/acs.jpcc.8b08913
J. Phys. Chem. C 2018, 122, 26499−26505

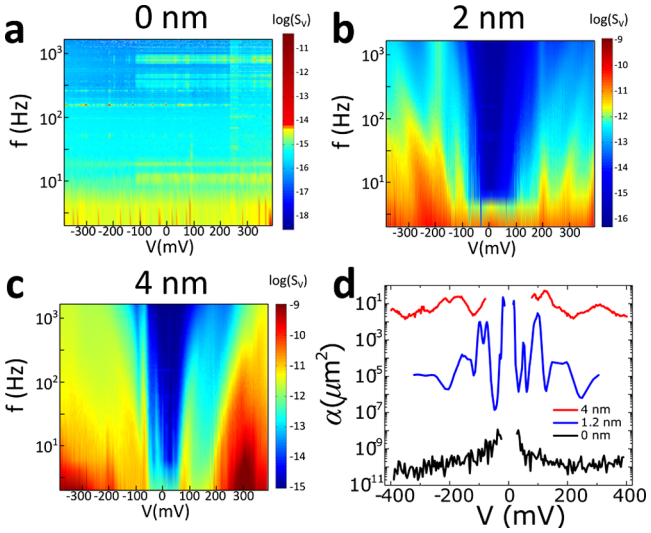

Figure 3. Noise spectroscopy of OMTJs in the P state as a function of PTCDA thickness. Part (a) shows the LFN spectra for control sample without PTCDA. Parts (b,c) show noise spectroscopy of OMTJ with 2 and 4 nm PTCDA correspondingly. Finally, part (d) shows variation of the bias-dependent LFN in OMTJs at different PTCDA thicknesses measured at T = 10 K and in the P state and quantified using the Hooge factor.

To show more clearly the applicability range of vibron noise spectroscopy when following the qualitative changes in the LFN with increasing PTCDA thickness, we may also use the Hooge factor explained in the Experimental Section. Figure 3d plots the bias dependence of the Hooge factor for OMTJs with three different PTCDA thicknesses. Although the control samples show a practically featureless Hooge versus bias dependence, the introduction of 1.2 nm PTCDA (about three PTCDA layers) between two ferromagnetic electrodes raises dramatically the normalized noise (several orders of magnitude). The strongest relative LFN anomalies with bias were observed for the 1.2−2 nm thick PTCDA barriers (Figure 3b,d). A further increase of the PTCDA thickness boosts the LFN background, approaching the LFN spectrum closer to the $1/f$ type. This induces a relative decrease of the magnitude of LFN anomalies, as seen for the OMTJs with 4 nm thick PTCDA. Generally, the evolution of LFN with PTCDA points toward a predominantly interfacial origin of the LFN anomalies, gradually affected by the accumulation of molecular disorder with an increasing barrier thickness.

It is important to note that magnetic-state dependent molecular vibron noise (Figure 2) in few orders of magnitude exceeds in the noise power expected from the application of fluctuation−dissipation theorem (FDT). Indeed, from FDT, the thermal noise power is[42] $S_V(f) = 4k_BTR$ (with T being temperature, R the junction resistance, and k_B the Boltzmann constant). Then, below 10 K with measured resistance change between P and AP state of few kiloohm, the noise power change expected from FDT should be less than $10^{-18}V^2$/Hz. The experimentally observed variation of the noise power between P and AP states (see Figure 2d) exceeds that by more than 6 orders of magnitude.

Concerning the robustness of the bias-dependent RTN anomalies in each magnetic state, we have carried out a number of reproducibility tests. The corresponding analysis shown in Figure S2 in the Supporting Information permits to conclude that the RTN versus bias anomalies are rather reproducible.

Interestingly, the enhancement of the LFN power at specific biases (up to several orders of magnitude) is accomplished with limited impact (with relative change below 10^{-2}) on the bias-dependent conductance (see Figure S3 in the Supporting Information). This suggests that a great majority of the molecular conductance channels in our OMTJs arise from well-established contacts between molecules and the electrodes. At the same time, only a small fraction of the total conductance channels (roughly estimated to be 10^{-2} to 10^{-3} from the relation between square root of the integrated over experimental bandwidth voltage noise power to the applied bias) forming hot spots contribute to the RTN as schematically sketched in Figure 1a.

4. DISCUSSION

On the basis of this scenario, we consider below a simple model of the barrier in which a molecular conduction pathway can attain two different states, for example, due to unavoidable interface roughness (Figure 4). The configuration becomes

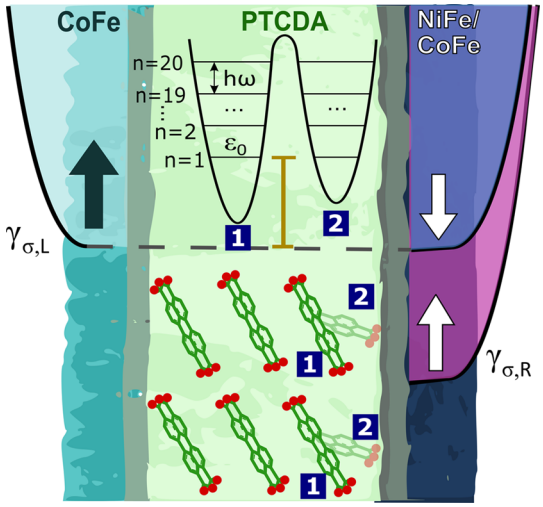

Figure 4. Sketch of a two-state switch driven by inelastic excitations by spin-polarized current. Although the microscopic origin is unknown, we speculate that they could correspond to molecules with incomplete or complete contact to the electrodes, respectively. Parabola-shaped lines with up/down arrows represent schematically majority and minority bands of the ferromagnetic electrodes. The two conformations are denoted as 1 and 2 in both the potential energy landscape (upper panel) and in real space (bottom panel). Also depicted are the main parameters of the model explained in the text such as one-electron energy ε_0; spin-dependent density of states for left (L) and right (R) electrodes correspondingly ($\gamma_{L,R}$); and vibrational levels n. The electrode spin polarization σ is depicted by the vertical arrows.

unstable under applied bias and switching between, for example, straight and bended molecular conformal configurations may occur. The stable conduction pathways (in parallel) contribute only to the background signal and provide practically a featureless $1/f$ noise. We therefore suggest that the observed excess of the RTN above certain characteristic biases is a result of inelastic excitations and conformational switching of individual molecules (or collective groups) in the barrier. We note that our model does not consider electron−electron correlations,[43] providing superpoissonian shot noise at low

DOI: 10.1021/acs.jpcc.8b08913
J. Phys. Chem. C 2018, 122, 26499−26505

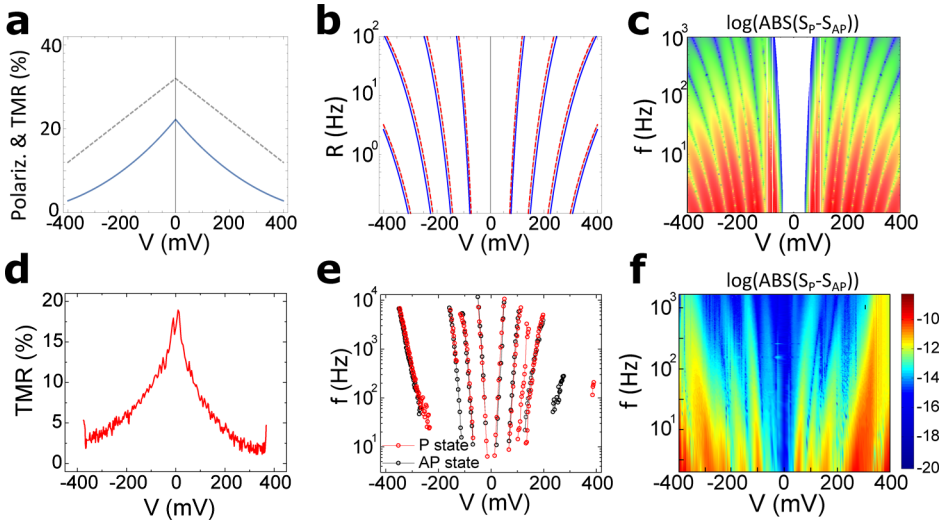

Figure 5. Comparison between LFN modeling and experiment for P and AP states. (a) Model for the electrode polarizations $\mathcal{P}_\alpha(V)$ (dotted gray line, eq S16 in the Supporting Information) and TMR (solid blue line, eq S22 in the Supporting Information) vs applied bias. (b) Calculated switching rates R in both P (dotted red line), AP (full blue line), and unpolarized (full gray line) cases. (c) Power noise spectrum difference between P and AP states in absolute value. Measurements of (d) TMR at T = 10 K, (e) RTN characteristic frequencies in P (red dots) and AP (black dots) states at T = 10 K, and (f) power noise spectrum at T = 0.3 K. Measurements were made in the 1.2 nm thick PTCDA sample.

(below 15 mW) biases, that is, when RTN is not yet activated.[36] This is because in the bias range under study (up to 400 mV), the total LFN power exceeds the shot noise contribution in more than the order of magnitude.[36]

Following refs,[44−46] we generalize a model for a two-state switch driven by inelastic excitations by a *spin-polarized* electronic current as detailed in the Supporting Information. Interestingly, this model predicts that the switching yield, that is, the probability that a tunneling electron induces the switching, is *larger* in the P than in the AP electrode configuration (Figure S6 in the Supporting Information). The origin of this effect is related to the available phase space (initial and final states) for the inelastic tunneling process, which is larger in P than in AP. This is analogous to the TMR effect where the elastic transmission of electrons is also larger in P than in AP. We note that these two effects compound in the switching rate R, cf. eq S19 in the Supporting Information.

To link these findings to the experimental observations, we present in Figure 5 an application of the model with appropriately chosen parameters. As detailed in the Supporting Information, we consider OMTJ as described by a single electronic resonance bridging two metal electrodes with coupling of the electrons to a set of vibrational modes on the molecular bridge. The numerical results shown in Figure 5 were obtained with the following model parameters defined in the Supporting Information: $\varepsilon_0 = 10\gamma_L = 10\gamma_R = 1$ eV, $n = 20$ and $\chi = 1$ meV. The molecular vibrations were described by a set of modes characterized by energies being multiples of $\hbar\Omega$ = 20 meV. The electrode polarization was defined phenomenologically as $\mathcal{P}_L = \pm\mathcal{P}_R = 0.32 - 0.5V^{-1}|V|$. The resulting TMR and LFN spectra $S(f)$ were computed using eqs S22 and S26 in the Supporting Information, respectively.

Figure 5a shows the electrode polarization (dashed gray curve) and TMR (blue curve), where the latter describes well the typical experimental voltage dependence of the TMR (Figure 5d). For simplicity, we represent the molecular vibrations by a set of modes characterized by energies being multiples of $\hbar\Omega$ = 20 meV. At a given applied voltage, this translates into a set of characteristic switching rates as shown in Figure 5b, qualitatively similar to the experimental data in Figure 5e. Finally, we analyze the magnetic-state dependent noise spectrum $S = S(V,f)$ for realistic bias-dependent TMRs and associated spin polarizations. By the eye, it is hard to appreciate the difference by P or AP (Figures 5b,e and S4 in the Supporting Information). The difference only becomes apparent when one considers the quantity $|S_P - S_{AP}|$ as shown in Figure 5c, in some resemblance with the experimental data in Figure 5f. We thus deduce that our modeling qualitatively can reproduce the main experimental observations.

5. CONCLUSIONS

In summary, we have introduced LFN spectroscopy as a tool to characterize buried organic−metal interfaces. Key elements for this spectroscopy are "hot spots" where molecular vibrational heating induces RTN detectable by standard noise measurement techniques. Moreover, we experimentally demonstrate and describe by the simple model the magnetic-state control of vibrational dynamics and switching in molecular spintronic devices. Our findings suggest the main LFN mechanism in molecular tunnel junctions with relatively ordered thin barriers and buried interfaces and therefore important for the development of reliable molecular spintronic devices.

■ ASSOCIATED CONTENT

Supporting Information

The Supporting Information is available free of charge on the ACS Publications website at DOI: 10.1021/acs.jpcc.8b08913.

Experimental data, reproducibility of the measurements, and theoretical model (PDF)

■ AUTHOR INFORMATION

Corresponding Author

*E-mail: farkhad.aliev@uam.es.

ORCID

Farkhad G. Aliev: 0000-0002-1682-3306

DOI: 10.1021/acs.jpcc.8b08913
J. Phys. Chem. C 2018, 122, 26499−26505

Author Contributions

[▽]I.M. and J.P.C. contributed equally.

Notes

The authors declare no competing financial interest.

■ ACKNOWLEDGMENTS

We thank Juan Carlos Cuevas, Stefano Sanvito, Gianaurelio Cuniberti, and Alex Dediu for stimulating discussions. The work in Madrid has been supported by Spanish MINECO (MAT2015-66000-P and EUIN2017-87474), Comunidad de Madrid (NANOFRONTMAG-CM S2013/MIT-2850), and IFIMAC (MDM-2014-0377). T.F. acknowledges FIS2017-83780-P from the Spanish MINECO. We also gratefully acknowledge the support by UAM-Santander collaborative project (2015/ASIA/04). J.P.C. acknowledges the support from the Fundacion Seneca (Region de Murcia) postdoctoral fellowship (19791/PD/15).

■ REFERENCES

(1) Mann, B.; Kuhn, H. Tunneling through Fatty Acid Salt Monolayers. *J. Appl. Phys.* **1971**, *42*, 4398−4405.
(2) Nitzan, A.; Ratner, M. A. Electron Transport in Molecular Wire Junctions. *Science* **2003**, *300*, 1384−1389.
(3) Galperin, M.; Ratner, M. A.; Nitzan, A. Molecular Transport Junctions: Vibrational Effects. *J. Phys.: Condens. Matter* **2007**, *19*, 103201.
(4) Kennehan, E. R.; Doucette, G. S.; Marshall, A. R.; Grieco, C.; Munson, K. T.; Beard, M. C.; Asbury, J. B. Electron-Phonon Coupling and Resonant Relaxation from 1D and 1P States in PbS Quantum Dots. *ACS Nano* **2018**, *12*, 6263−6272.
(5) Chen, J.; Isshiki, H.; Baretzky, C.; Balashov, T.; Wulfhekel, W. Abrupt Switching of Crystal Fields during Formation of Molecular Contacts. *ACS Nano* **2018**, *12*, 3280−3286.
(6) Santos, T. S.; Lee, J. S.; Migdal, P.; Lekshmi, I. C.; Satpati, B.; Moodera, J. S. Room-Temperature Tunnel Magnetoresistance and Spin-Polarized Tunneling through an Organic Semiconductor Barrier. *Phys. Rev. Lett.* **2007**, *98*, 016601.
(7) Li, K.-S.; Chang, Y.-M.; Agilan, S.; Hong, J.-Y.; Tai, J.-C.; Chiang, W.-C.; Fukutani, K.; Dowben, P. A.; Lin, M.-T. Organic Spin Valves with Inelastic Tunneling Characteristics. *Phys. Rev. B: Condens. Matter Mater. Phys.* **2011**, *83*, 172404.
(8) Wiktor, C.; Meledina, M.; Turner, S.; Lebedev, O. I.; Fischer, R. A. Transmission Electron Microscopy on Metal−Organic Frameworks—a Review. *J. Mater. Chem. A* **2017**, *5*, 14969−14989.
(9) Galperin, M.; Ratner, M. A.; Nitzan, A. Hysteresis, Switching, and Negative Differential Resistance in Molecular Junctions: a Polaron Model. *Nano Lett.* **2005**, *5*, 125−130.
(10) Ward, D. R.; Corley, D. A.; Tour, J. M.; Natelson, D. Vibrational and Electronic Heating in Nanoscale Junctions. *Nat. Nanotechnol.* **2011**, *6*, 33−38.
(11) Elliott, A. B. S.; Horvath, R.; Gordon, K. C. Vibrational Spectroscopy as a Probe of Molecule-Based Devices. *Chem. Soc. Rev.* **2012**, *41*, 1929−1946.
(12) Galbiati, M.; Tatay, S.; Delprat, S.; Khanh, H. L.; Servet, B.; Deranlot, C.; Collin, S.; Seneor, P.; Mattana, R.; Petroff, F. Is Spin Transport through Molecules really occurring in Organic Spin Valves? A Combined Magnetoresistance and Inelastic Electron Tunnelling Spectroscopy Study. *Appl. Phys. Lett.* **2015**, *106*, 082408.
(13) Tan, Y.; Ma, L.; Gao, Z.; Chen, M.; Chen, F. Two-Dimensional Heterostructure as a Platform for Surface-Enhanced Raman Scattering. *Nano Lett.* **2017**, *17*, 2621−2626.
(14) Jaklevic, R. C.; Lambe, J. Molecular Vibration Spectra by Electron Tunneling. *Phys. Rev. Lett.* **1966**, *17*, 1139−1140.
(15) Stipe, B. C.; Rezaei, M. A.; Ho, W. Single-Molecule Vibrational Spectroscopy and Microscopy. *Science* **1998**, *280*, 1732−1735.
(16) Smit, R. H. M.; Noat, Y.; Untiedt, C.; Lang, N. D.; van Hemert, M. C.; van Ruitenbeek, J. M. Measurement of the Conductance of a Hydrogen Molecule. *Nature* **2002**, *419*, 906−909.
(17) Heinrich, A. J.; Gupta, J. A.; Lutz, C. P.; Eigler, D. M. Single-Atom Spin-Flip Spectroscopy. *Science* **2004**, *306*, 466−469.
(18) Delgado, F.; Fernández-Rossier, J. Spin Dynamics of Current-driven Single Magnetic Adatoms and Molecules. *Phys. Rev. B: Condens. Matter Mater. Phys.* **2010**, *82*, 134414.
(19) Dubi, Y.; Di Ventra, M. Colloquium: Heat flow and Thermoelectricity in Atomic and Molecular Junctions. *Rev. Mod. Phys.* **2011**, *83*, 131−155.
(20) Simine, L.; Segal, D. Vibrational Cooling, Heating, and Instability in Molecular Conducting Junctions: Full Counting Statistics Analysis. *Phys. Chem. Chem. Phys.* **2012**, *14*, 13820−13834.
(21) Weiss, S.; Brüggemann, J.; Thorwart, M. Spin Vibronics in Interacting Nonmagnetic Molecular Nanojunctions. *Phys. Rev. B: Condens. Matter Mater. Phys.* **2015**, *92*, 045431.
(22) Galperin, M.; Saito, K.; Balatsky, A. V.; Nitzan, A. Cooling Mechanisms in Molecular Conduction Junctions. *Phys. Rev. B: Condens. Matter Mater. Phys.* **2009**, *80*, 115427.
(23) Dediu, V.; Murgia, M.; Matacotta, F. C.; Taliani, C.; Barbanera, S. Room Temperature Spin Polarized Injection in Organic Semiconductor. *Solid State Commun.* **2002**, *122*, 181−184.
(24) Xiong, Z. H.; Wu, D.; Valy Vardeny, Z.; Shi, J. Giant magnetoresistance in organic spin-valves. *Nature* **2004**, *427*, 821−824.
(25) Rocha, A. R.; García-suárez, V. M.; Bailey, S. W.; Lambert, C. J.; Ferrer, J.; Sanvito, S. Towards Molecular Spintronics. *Nat. Mater.* **2005**, *4*, 335−339.
(26) Sanvito, S. Molecular Spintronics. *Chem. Soc. Rev.* **2011**, *40*, 3336−3355.
(27) Jiang, J. S.; Pearson, J. E.; Bader, S. D. Direct Determination of Energy Level Alignment and Charge Transport at Metal−Alq3 Interfaces via Ballistic-Electron-Emission Spectroscopy. *Phys. Rev. Lett.* **2011**, *106*, 156807.
(28) Vincent, R.; Klyatskaya, S.; Ruben, M.; Wernsdorfer, W.; Balestro, F. Electronic Read-out of a Single Nuclear Spin using a Molecular Spin Transistor. *Nature* **2012**, *488*, 357−360.
(29) Nguyen, T. D.; Ehrenfreund, E.; Vardeny, Z. V. Spin-Polarized Light-Emitting Diode Based on an Organic Bipolar Spin Valve. *Science* **2012**, *337*, 204−209.
(30) Rakhmilevitch, D.; Sarkar, S.; Bitton, O.; Kronik, L.; Tal, O. Enhanced Magnetoresistance in Molecular Junctions by Geometrical Optimization of Spin-Selective Orbital Hybridization. *Nano Lett.* **2016**, *16*, 1741−1745.
(31) Sanvito, S. The rise of spinterface science. *Nat. Phys.* **2010**, *6*, 562−564.
(32) Lach, S.; Altenhof, A.; Tarafder, K.; Schmitt, F.; Ali, M. E.; Vogel, M.; Sauther, J.; Oppeneer, P. M.; Ziegler, C. Metal-Organic Hybrid Interface States of A Ferromagnet/Organic Semiconductor Hybrid Junction as Basis For Engineering Spin Injection in Organic Spintronics. *Adv. Funct. Mater.* **2012**, *22*, 989−997.
(33) Droghetti, A.; Rungger, I.; Cinchetti, M.; Sanvito, S. Vibron-assisted Spin Relaxation at a Metal/Organic Interface. *Phys. Rev. B: Condens. Matter Mater. Phys.* **2015**, *91*, 224427.
(34) Lunghi, A.; Totti, F.; Sessoli, R.; Sanvito, S. The Role of Anharmonic Phonons in under-barrier Spin Relaxation of Single Molecule Magnets. *Nat. Commun.* **2017**, *8*, 14620.
(35) Shin, D.; Hübener, H.; De Giovannini, U.; Jin, H.; Rubio, A.; Park, N. Phonon-driven Spin-Floquet Magneto-valleytronics in MoS2. *Nat. Commun.* **2018**, *9*, 638.
(36) Cascales, J. P.; Hong, J.-Y.; Martinez, I.; Lin, M.-T.; Szczepański, T.; Dugaev, V. K.; Barnaś, J.; Aliev, F. G. Super-poissonian Shot Noise in Organic Magnetic Tunnel Junctions. *Appl. Phys. Lett.* **2014**, *105*, 233302.
(37) Tsutsui, M.; Taniguchi, M.; Kawai, T. Single-molecule Identification via Electric Current Noise. *Nat. Commun.* **2010**, *1*, 138.
(38) Schaffert, J.; Cottin, M. C.; Sonntag, A.; Karacuban, H.; Bobisch, C. A.; Lorente, N.; Gauyacq, J.-P.; Möller, R. Imaging the

DOI: 10.1021/acs.jpcc.8b08913
J. Phys. Chem. C 2018, 122, 26499−26505

Dynamics of Individually Adsorbed Molecules. *Nat. Mater.* **2012**, *12*, 223−227.
(39) Hong, J.-Y.; Ou Yang, K.-H.; Wang, B.-Y.; Li, K.-S.; Shiu, H.-W.; Chen, C.-H.; Chan, Y.-L.; Wei, D.-H.; Chang, F.-H.; Lin, H.-J.; Chiang, W.-C.; Lin, M.-T. Interfacial Spectroscopic Characterization of Organic/Ferromagnet Hetero-junction of 3,4,9,10-perylene-teracarboxylic dianhydride-based Organic Spin Valves. *Appl. Phys. Lett.* **2014**, *104*, 083301.
(40) Herranz, D.; Bonell, F.; Gomez-Ibarlucea, A.; Andrieu, S.; Montaigne, F.; Villar, R.; Tiusan, C.; Aliev, F. G. Strongly suppressed 1/f noise and enhanced magnetoresistance in epitaxial Fe-V/MgO/Fe magnetic tunnel junctions. *Appl. Phys. Lett.* **2010**, *96*, 202501.
(41) Clement, N.; Pleutin, S.; Seitz, O.; Lenfant, S.; Vuillaume, D. 1/f Tunnel Current Noise through Si-bound Alkyl Monolayers. *Phys. Rev. B: Condens. Matter Mater. Phys.* **2007**, *76*, 205407.
(42) Aliev, F. G.; Cascales, J. P. *Noise in Spintronics: From Understanding to Manipulation*; Pan Stanford Publishing: Singapore, 2018.
(43) Aliev, F. G.; Kunnen, E.; Temst, K.; Mae, K.; Verbanck, G.; Barnas, J.; Moshchalkov, V. V.; Bruynseraede, Y. Periodic Enhancement of the Electron-Electron Interactions and the Magnetoresistance in Magnetic Co/(Cr/Ag)/Co Multilayers. *Phys. Rev. Lett.* **1997**, *78*, 134−137.
(44) Gao, S.; Persson, M.; Lundqvist, B. I. Theory of Atom Transfer with a Scanning Tunneling Microscope. *Phys. Rev. B: Condens. Matter Mater. Phys.* **1997**, *55*, 4825−4836.
(45) Brumme, T.; Gutierrez, R.; Cuniberti, G. Vibrational Heating in Single-molecule Switches: an Energy-dependent Density-of-states approach. *J. Phys.: Condens. Matter* **2012**, *24*, 394003.
(46) Frederiksen, T.; Paulsson, M.; Ueba, H. Theory of Action Spectroscopy for Single-molecule Reactions induced by Vibrational Excitations with STM. *Phys. Rev. B: Condens. Matter Mater. Phys.* **2014**, *89*, 035427.

DOI: 10.1021/acs.jpcc.8b08913
J. Phys. Chem. C 2018, 122, 26499−26505